CAPACITY ANALYSIS FOR PARALLEL AND SEQUENTIAL MIMO EQUALIZERS

Xinying Zhang and S. Y. Kung

Princeton University

ABSTRACT

It is well known that linear MMSE can outperform its zero-forcing counterpart. In combination with a successive interference canceller, MMSE can fully exploit the capacity of MIMO (Multiple-Input-Multiple-Output) channels [1, 2]. In practice, however, such an advantage is compromised due to its implementation complexity and the requirement of accurate SNR estimate. Thus other equalizers such as zero-forcing may present an attractive alternative as long as the performance gap is tolerable. This motivates a need to quantify the tradeoff between MMSE and zero-forcing in both parallel and sequential structures. In this paper, the capacity performance of different equalization schemes is investigated, with closed-form formulas provided in terms of two key measures: capacity gaps and ratios. We also conclude that the capacity gain via structural choice (between parallel and sequential) far out-weights that via filter choice (between zero-forcing and MMSE). Indeed, the latter is found to be almost negligible for most practical SNR regions. It is also shown that the sequential zero-forcing equalizers can asymptotically reach the channel capacity when SNR approaches infinity, irrelevant of the detection order. Although this paper is focused on the flat-fading channels, the result is directly extendable to the ISI case by slicing the frequency band into infinitesimal stripes, each of which can be treated as flat.

1. MATHEMATICAL CHANNEL MODEL

We consider a general MIMO communication system adopting t transmit and r receive antenna elements:

$$\vec{x}(k) = \mathbf{H}\vec{s}(k) + \vec{n}(k) \tag{1}$$

where $\vec{x}(k) \in \mathcal{C}^r$, $\vec{s}(k) \in \mathcal{C}^t$ are sample stacks of the complex-valued receiver data and transmission sequences, and $\mathbf{H}$ is the $r \times t$ channel transfer function. The total transmission power is constrained to P and is shared by the t transmitting antennas with distribution factors $\{\phi_1, \ldots, \phi_t\}$: $E[s_i(k)s_i^\dagger(k)] = \phi_i P$, where $\sum_{i=1}^t \phi_i = 1$. The thermal noises $\vec{n}(k) \in \mathcal{C}^r$ are both spatially and temporally white i.i.d Gaussian random processes with independent real and imaginary parts and variance $N\mathbf{I}_r$. Assuming independent inputs, the capacity of the MIMO system in (1) is well known as

$$\begin{aligned} C &= \log_2 \det(\mathbf{I}_r + \frac{P}{N}\mathbf{H}\mathbf{\Phi}\mathbf{H}^\dagger) \\ &= \log_2 \det(\mathbf{I}_t + \rho\mathbf{\Phi}^{1/2}\mathbf{H}^\dagger\mathbf{H}\mathbf{\Phi}^{1/2}) \\ &= \sum_{i=1}^{t} \log_2(1 + \rho|\lambda_i|^2) \end{aligned} \tag{2}$$

This research was supported in part by a grant from Mitsubishi Electric Research Laboratories.

where $\mathbf{\Phi} = diag\{\phi_i\}_{i=1}^t$, $\rho = \frac{P}{N}$ is the nominal signal to noise ratio and $\{|\lambda_i|^2\}_{i=1}^t$ are the singular values of $\mathbf{\Phi}^{1/2}\mathbf{H}^\dagger\mathbf{H}\mathbf{\Phi}^{1/2}$. Here † denotes the conjugate transpose of a matrix (vector). In this paper, we assume that $r \geq t$ and the channel is generic, i.e. $\mathbf{H}$ has full column rank. The channel realization is assumed to be tracked at the receiver end.

2. PARALLEL LINEAR MIMO EQUALIZERS

2.1. Parallel Zero-Forcing (ZF) Equalizers

For the recovery of ith input stream $s_i(k)$, the zero-forcing constraint on the corresponding diversity-combiner, denoted by the row vector $\vec{g}_{ZF,i}$, is

$$\vec{g}_{ZF,i}\mathbf{H} = \vec{e}_i \tag{3}$$

where $\vec{e}_i$ is a unit (row) vector with all elements zero except 1 at position i. Specifically, the application of $\vec{g}_{ZF,i}$ in (3) yields a virtual SISO (Single-Input-Single-Output) channel

$$\vec{g}_{ZF,i}\vec{x}(k) = s_i(k) + \vec{g}_{ZF,i}\vec{n}(k) \tag{4}$$

with the associated capacity

$$C_{ZF,i} = \log_2(1 + \frac{\phi_i\rho}{\|\vec{g}_{ZF,i}\|^2}). \tag{5}$$

Simultaneous application of these t filters on the receiver data yields a parallel structure, whereafter the original MIMO is converted into t independent and interference-free channels that can be separately decoded. The total information rate supported by the parallel ZF equalization is therefore the summation of the sub-channel capacities $C_{ZF,i}$ over all the indices $i = 1, \ldots, t$. The optimal parallel ZF equalizers satisfying (3) and maximizing (5) are given by

$$\vec{g}_{ZF,i} = \vec{e}_i\mathbf{H}^+, \quad i = 1, \ldots, t, \tag{6}$$

where $\mathbf{H}^+$ denotes the left pseudo-inverse of $\mathbf{H}$.

We introduce the following Cholesky factorization:

$$\mathbf{\Phi}^{1/2}\mathbf{H}^\dagger\mathbf{H}\mathbf{\Phi}^{1/2} = \mathbf{R}^\dagger\mathbf{R} \tag{7}$$

where $\mathbf{R} = [r_{ij}]$ is a nonsingular upper-triangular matrix. It turns out that the quantitative analysis hinges upon the inverse matrix $\mathbf{R}^{-1}$, especially the two sets of correlation factors defined below:

$$\begin{aligned} \alpha_i &= |r_{ii}|^2\|\vec{e}_i\mathbf{R}^{-1}\|^2 - 1 \geq 0 \\ \beta_i &= \frac{\|\vec{e}_i\mathbf{R}^{-1}\mathbf{R}^{-\dagger}\|^2}{\|\vec{e}_i\mathbf{R}^{-1}\|^4} - 1 \geq 0. \end{aligned}$$

Note that the parameters α_i and β_i represent the degree of correlation between the channel vectors regarding different inputs. They are respectively the 2-norm ratio of the total off-diagonal terms to the diagonal terms in the ith row of matrix $\mathbf{R}^{-1}$ and $\mathbf{R}^{-1}\mathbf{R}^{-\dagger}$. In fact, $\{\ \alpha_i\ \}$ depend only on the channel transfer function $\mathbf{H}$, while $\{\ \beta_i\ \}$ depend on both $\mathbf{H}$ and $\mathbf{\Phi}$.

Theorem 1 (Capacity Gap of Parallel ZF Equalizers) *In high SNR region, the asymptotic gap between the original MIMO channel capacity and the achievable capacity of the optimal parallel ZF equalizers in (6) is*

$$C - C_{ZF} = \sum_{i=1}^{t} \log_2(1+\alpha_i) + O(\rho^{-2}). \quad (8)$$

Proof: By (5) and (6), the capacity performance of the optimal ZF equalizers is

$$\begin{aligned} C_{ZF} &= \sum_{i=1}^{t} \log_2(1+\frac{\phi_i\rho}{\|\vec{g}_{ZF,i}\|^2}) \\ &= \sum_{i=1}^{t} \log_2[1+\frac{\rho}{\vec{e}_i(\mathbf{\Phi}^{1/2}\mathbf{H}^\dagger\mathbf{H}\mathbf{\Phi}^{1/2})^{-1}\vec{e}_i^\dagger}] \\ &= \sum_{i=1}^{t} \log_2[1+\frac{\rho}{\vec{e}_i(\mathbf{R}^\dagger\mathbf{R})^{-1}\vec{e}_i^\dagger}] \\ &= \sum_{i=1}^{t} \log_2(1+\frac{\rho|r_{ii}|^2}{1+\alpha_i}). \quad (9) \end{aligned}$$

Compare (9) with the original MIMO capacity in (2), we have

$$\begin{aligned} C - C_{ZF} &= \sum_{i=1}^{t} \log_2(1+\alpha_i) + \sum_{i=1}^{t} \log_2 \frac{|\lambda_i|^2}{|r_{ii}|^2} \\ &+ \sum_{i=1}^{t} \log_2 \frac{1+\frac{1}{|\lambda_i|^2\rho}}{1+\frac{1+\alpha_i}{\rho|r_{ii}|^2}}. \quad (10) \end{aligned}$$

As $\{|\lambda_i|^2\}_{i=1}^t$ are the singular values for the Hermitian matrix $\mathbf{\Phi}^{1/2}\mathbf{H}^\dagger\mathbf{H}\mathbf{\Phi}^{1/2} = \mathbf{R}^\dagger\mathbf{R}$, we have

$$\begin{aligned} \prod_{i=1}^{t}|\lambda_i|^2 &= \det[\mathbf{R}^\dagger\mathbf{R}] = \prod_{i=1}^{t}|r_{ii}|^2 \\ \sum_{i=1}^{t}\frac{1}{|\lambda_i|^2} &= tr[(\mathbf{R}^\dagger\mathbf{R})^{-1}] = \sum_{i=1}^{t}\frac{1+\alpha_i}{|r_{ii}|^2}. \quad (11) \end{aligned}$$

With the two equalities above, when $\rho \gg 1$, the capacity gap in (10) is simplified as

$$C - C_{ZF} = \sum_{i=1}^{t} \log_2(1+\alpha_i) + O(\rho^{-2}) \quad (12)$$

by using $\log_2(1+x) = \frac{x}{\ln 2} + O(x^2)$ for small x.

2.2. Parallel MMSE Equalizers

Qualitatively, it is well known that MMSE can outperform its zero-forcing counterpart. In this section, we shall investigate the quantitative aspect of this improvement. The individual MMSE filter for input i is

$$\vec{g}_{M,i} = \rho\vec{e}_i\mathbf{\Phi}^{1/2}\mathbf{H}^\dagger(\mathbf{I}+\rho\mathbf{H}\mathbf{\Phi}\mathbf{H}^\dagger)^{-1}. \quad (13)$$

After the application of $\vec{g}_{M,i}$ on the receiver data $\vec{x}(k)$, the SIR (Signal-to-Interference-Ratio) is

$$\begin{aligned} SIR &= \frac{\rho|\vec{g}_{M,i}\mathbf{H}\mathbf{\Phi}^{1/2}\vec{e}_i^\dagger|^2}{\vec{g}_{M,i}(\mathbf{I}+\rho\mathbf{H}\mathbf{\Xi_i}\mathbf{\Phi}\mathbf{\Xi_i}\mathbf{H}^\dagger)\vec{g}_{M,i}^\dagger} \\ &= \rho\vec{e}_i\mathbf{\Phi}^{1/2}\mathbf{H}^\dagger(\mathbf{I}+\rho\mathbf{H}\mathbf{\Xi_i}\mathbf{\Phi}\mathbf{\Xi_i}\mathbf{H}^\dagger)^{-1}\mathbf{H}\mathbf{\Phi}^{1/2}\vec{e}_i^\dagger \quad (14) \end{aligned}$$

where $\mathbf{\Xi}_i$ denotes the identity matrix with ith diagonal element equal to zero. The corresponding capacity achieved in each equalized sub-channel is therefore

$$\begin{aligned} &\log_2(1+SIR) \\ =\ &-\log_2\{\vec{e}_i[\mathbf{I}-\rho\mathbf{\Phi}^{1/2}\mathbf{H}^\dagger(\mathbf{I}+\rho\mathbf{H}\mathbf{\Phi}\mathbf{H}^\dagger)^{-1}\mathbf{H}\mathbf{\Phi}^{1/2}]\vec{e}_i^\dagger\} \\ =\ &-\log_2[\vec{e}_i(\mathbf{I}+\rho\mathbf{\Phi}^{1/2}\mathbf{H}^\dagger\mathbf{H}\mathbf{\Phi}^{1/2})^{-1}\vec{e}_i^\dagger]. \quad (15) \end{aligned}$$

The equalities above can be obtained via the Sherman-Morrison-Woodbury Identity.

Theorem 2 (Improvement of Parallel MMSE Equalizers) *In high SNR region, the difference of the achievable capacity between parallel MMSE and ZF equalizers is*

$$C_{MMSE} - C_{ZF} = \rho^{-1}\sum_{i=1}^{t}\frac{\beta_i(1+\alpha_i)}{|r_{ii}|^2} + O(\rho^{-2}). \quad (16)$$

Proof: Comparing equations (9) and (15), the gap is

$$\begin{aligned} &C_{MMSE,i} - C_{ZF,i} \\ =\ &\log_2\frac{1}{\vec{e}_i(\mathbf{I}+\rho\mathbf{R}^\dagger\mathbf{R})^{-1}\vec{e}_i^\dagger(1+\frac{\rho}{\vec{e}_i(\mathbf{R}^\dagger\mathbf{R})^{-1}\vec{e}_i^\dagger})}. \quad (17) \end{aligned}$$

Note that for large ρ,

$$\begin{aligned} &\vec{e}_i(\mathbf{I}+\rho\mathbf{R}^\dagger\mathbf{R})^{-1}\vec{e}_i^\dagger \\ =\ &\vec{e}_i(\rho\mathbf{R}^\dagger\mathbf{R})^{-1}[\mathbf{I}+(\rho\mathbf{R}^\dagger\mathbf{R})^{-1}]^{-1}\vec{e}_i^\dagger \\ =\ &\vec{e}_i[\rho^{-1}(\mathbf{R}^\dagger\mathbf{R})^{-1}-\rho^{-2}(\mathbf{R}^\dagger\mathbf{R})^{-2}]\vec{e}_i^\dagger + O(\rho^{-3}) \\ \Longrightarrow\ &C_{MMSE,i} - C_{ZF,i} \\ =\ &\rho^{-1}[\frac{\vec{e}_i(\mathbf{R}^\dagger\mathbf{R})^{-2}\vec{e}_i^\dagger}{\vec{e}_i(\mathbf{R}^\dagger\mathbf{R})^{-1}\vec{e}_i^\dagger} - \vec{e}_i(\mathbf{R}^\dagger\mathbf{R})^{-1}\vec{e}_i^\dagger] + O(\rho^{-2}) \\ =\ &\rho^{-1}\frac{\beta_i(1+\alpha_i)}{|r_{ii}|^2} + O(\rho^{-2}). \quad (18) \end{aligned}$$

Theorems 1 and 2 show an asymptotically constant capacity degradation of $\sum_{i=1}^{t}\log_2(1+\alpha_i)$ for both the linear MMSE and ZF schemes. (Thus this gap is a function of $\mathbf{H}$ only.) The channel capacity can be asymptotically achieved only when *all* the channel correlation factors $\alpha_i = 0$, which is rarely the case in practice. However, as discussed in the subsequent section, the degradation caused by such correlations can be artificially eliminated via a successive interference cancellation procedure.

3. SEQUENTIAL ZERO-FORCING (SZF) EQUALIZERS

In BLAST design [3], Foschini proved that the successive ZF can asymptotically approach the capacity lower bound for Rayleigh fading MIMOs when $r = t$. In this section, we give a comprehensive capacity analysis of SZF equalizers in the entire SNR range for any channel realization and antenna settings.

For notational simplicity, we assume that the input streams are sequentially retrieved in the order of $t, t-1, \ldots, 1$. In the SZF equalizer, the detected input stream can be used to help the detection of others via decision feedback. The interferences generated by the already-detected inputs are successively nulled from the observation data before the equalizers for the other inputs are applied.

Assuming no error propagation, the interference-reduced receiver data, at the input of ith individual equalizer, is:

$$\vec{x}^{(i)}(k) = \mathbf{H}_i \vec{s}^{(i)}(k) + \vec{n}(k) \tag{19}$$

where $\mathbf{H}_i$ is the first i columns of $\mathbf{H}$ denoting the virtual channel after the inputs $i+1, i+2, \ldots, t$ have been detected and eliminated. The vector $\vec{s}^{(i)}(k)$ is the first i rows of $\vec{s}(k)$. The ZF constraint for the sequential equalizers is now

$$\vec{g}_{SZF,i}\mathbf{H}_i = \vec{e}_i, \quad 1 \le i \le t. \tag{20}$$

Also we denote $\mathbf{R}_i(\mathbf{\Phi}_i)$ as the left-upper $i \times i$ minors of $\mathbf{R}(\mathbf{\Phi})$. Exploiting the upper-triangular structure of $\mathbf{R}$, we get

$$\mathbf{\Phi}_i^{1/2}\mathbf{H}_i^\dagger \mathbf{H}_i \mathbf{\Phi}_i^{1/2} = \mathbf{R}_i^\dagger \mathbf{R}_i. \tag{21}$$

Theorem 3 (Capacity Gap and Ratio for SZF Equalizers)
The gap between the channel capacity and that achieved by the optimal SZF is:

$$C - C_{SZF} = \sum_{i=1}^{t} \log_2 \frac{1+\rho|\lambda_i|^2}{1+\rho|r_{ii}|^2}. \tag{22}$$

1. *In high SNR region:*

$$\begin{aligned} \frac{C_{SZF}}{C} &= 1 - \frac{1}{t\rho \ln \rho}\sum_{i=1}^{t}\frac{\alpha_i}{|r_{ii}|^2} + o[(\rho \ln \rho)^{-1}] \\ C - C_{SZF} &= \frac{\rho^{-1}}{\ln 2}\sum_{i=1}^{t}\frac{\alpha_i}{|r_{ii}|^2} + O(\rho^{-2}); \end{aligned} \tag{23}$$

2. *In low SNR region:*

$$\begin{aligned} C - C_{SZF} &= \frac{\rho}{\ln 2}(tr[\mathbf{R}^\dagger\mathbf{R}] - \sum_{i=1}^{t}|r_{ii}|^2) + O(\rho^2) \\ \frac{C_{SZF}}{C} &= \frac{\sum_{i=1}^{t}|r_{ii}|^2}{tr[\mathbf{R}^\dagger\mathbf{R}]} + O(\rho). \end{aligned} \tag{24}$$

Proof: Just like the parallel case, the optimal SZF equalizers $\vec{g}_{SZF,i}$ satisfying the constraint (20) is

$$\vec{g}_{SZF,i} = \vec{e}_i \mathbf{H}_i^+ \tag{25}$$

with the corresponding capacity

$$\begin{aligned} C_{SZF} &= \sum_{i=1}^{t} C_{SZF,i} = \sum_{i=1}^{t}\log_2[1 + \frac{\rho\phi_i}{\|\vec{g}_{SZF,i}\|^2}] \\ &= \sum_{i=1}^{t}\log_2[1 + \frac{\rho}{\vec{e}_i(\mathbf{\Phi}_i^{1/2}\mathbf{H}_i^\dagger\mathbf{H}_i\mathbf{\Phi}_i^{1/2})^{-1}\vec{e}_i^\dagger}] \\ &= \sum_{i=1}^{t}\log_2[1 + \frac{\rho}{\vec{e}_i\mathbf{R}_i^{-1}\mathbf{R}_i^{-\dagger}\vec{e}_i^\dagger}] \\ &= \sum_{i=1}^{t}\log_2(1+\rho|r_{ii}|^2). \end{aligned} \tag{26}$$

The capacity gap is

$$\begin{aligned} C - C_{SZF} &= \sum_{i=1}^{t}\log_2\frac{1+\rho|\lambda_i|^2}{1+\rho|r_{ii}|^2} \\ &= \sum_{i=1}^{t}\log_2\frac{1+\frac{1}{\rho|\lambda_i|^2}}{1+\frac{1}{\rho|r_{ii}|^2}} + \sum_{i=1}^{t}\log_2\frac{|\lambda_i|^2}{|r_{ii}|^2} \end{aligned} \tag{27}$$

In large SNR region, by applying (11) we obtain the 1st order expansion

$$C - C_{SZF} = \frac{\rho^{-1}}{\ln 2}\sum_{i=1}^{t}\frac{\alpha_i}{|r_{ii}|^2} + O(\rho^{-2}). \tag{28}$$

The other derivations are basically similar (omitted here).

Theorem 4 (Capacity Achieving Property of SZF)
The SZF asymptotically achieves the original channel capacity when the SNR ρ goes toward either infinity or zero: $C_{SZF} \doteq C$. It holds true irrelevant of the detection order.

Proof: The capacity-achieving claim is obvious with reference to (23) and (24). When $\rho \to \infty$, (26) leads to

$$C_{SZF} \doteq C \doteq \sum_{i=1}^{t}\log_2(\rho|r_{ii}|^2) = \log_2\rho^t \det[\mathbf{R}^\dagger\mathbf{R}]. \tag{29}$$

Assume that the t input streams are to be retrieved in a different order. This can be accomplished by rearranging the columns of $\mathbf{H}$ by a permutation matrix $\mathbf{P}$, i.e. $\mathbf{H}' = \mathbf{HP}$. Accordingly, $\mathbf{\Phi}' = \mathbf{\Phi P}$. Denote $\mathbf{R}'$ as the Cholesky factorization matrices of $(\mathbf{\Phi}')^{1/2}(\mathbf{H}')^\dagger\mathbf{H}'(\mathbf{\Phi}')^{1/2}$. Based on (29), the proof is completed by noting that $\mathbf{PP}^\dagger = \mathbf{I}_t$ and hence

$$\det[(\mathbf{R}')^\dagger\mathbf{R}'] = \det[\mathbf{R}^\dagger\mathbf{R}]. \tag{30}$$

Remark 1 *Empirically, the capacity ratio $\frac{C_{SZF}}{C}$ is a monotonically increasing function of ρ for all generic channels (i.e. when $\frac{\min(|\lambda_i|^2)}{\max(|\lambda_i|^2)}$ is above certain QoS-safeguard threshold). In fact, the range of capacity ratio runs roughly from γ (when $\rho \to 0$) to 1.0 (when $\rho \to \infty$), where*

$$\gamma = \frac{\sum_{i=1}^{t}|r_{ii}|^2}{tr[\mathbf{R}^\dagger\mathbf{R}]}.$$

Note that though the effect of channel coupling α_i is eliminated for large SNR (i.e. $\frac{C_{SZF}}{C} \to 1$ as $\rho \to \infty$), it still has impact on the SZF performance when SNR is small through another factor γ. For an ill-conditioned system with highly aligned channel vectors (inducing some very small singular values λ_i), the correlation between different antenna channels can be severe and lead to a small-valued γ.

Remark 2 *It was known that sequential MMSE equalizers can achieve the full channel capacity in the entire SNR range [1, 2], provided an accurate SNR estimate. Theorems 2 and 3 demonstrate that the capacity advantage of MMSE over ZF is not significant in most practical SNR regions. Quantitatively speaking, their difference is in the order of ρ^{-1} for high SNR. Note also that the most complex operation in these equalizer designs are those involving matrix inversions (or Cholesky decompositions). Parallel ZF, parallel MMSE, and SZF equalizers all require only one matrix inversion for the t users while the sequential MMSE would require t such operations. Altogether, it appears that SZF equalizers represent an attractive solution since they can deliver very satisfactory performance while incurring minimum complexity overhead.*

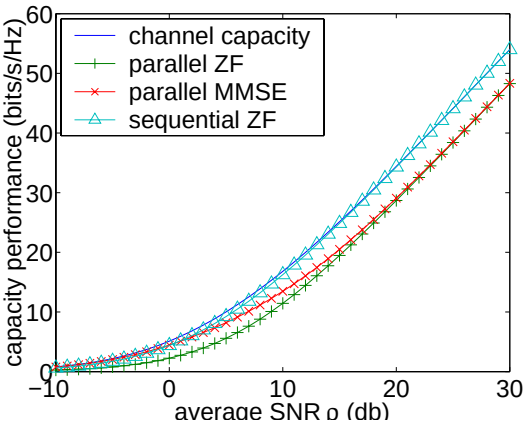

Fig. 1. Capacity performance comparison for different equalizers. For $\rho \geq 10db$, the importance of the structural choice (parallel vs. sequential) far exceeds the filter choice (ZF vs. MMSE).

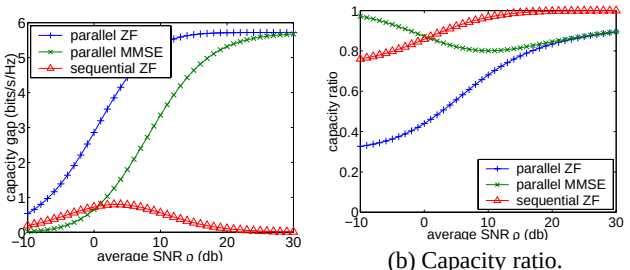

(a) Capacity gap. (b) Capacity ratio.

Fig. 2. Comparison of (a) capacity gap (b) capacity ratio for different equalizers. Asymptotically, only SZF approaches a zero capacity gap as ρ increases.

4. SIMULATION

Simulations are conducted to verify the theoretical analysis. First we simulate a randomly generated 6-input-6-output channel with even power distribution, and the Frobenius norm of the transfer function is normalized to $t \times r = 36$, i.e. $\|H\|_F^2 = 36$. Therefore the nominal SNR ρ represents the average signal to noise ratio at each receiver. The capacity performance of different equalizers under a typical channel realization is displayed with respect to ρ. The constant capacity gaps of parallel ZF or MMSE (illustrated by the two lower curves in Figure 1) when ρ is large consolidate our finding in Theorems 1 and 2. For clarity, such capacity gaps and ratios are magnified in Figure 2. The shapes of these curves again agree to our closed-form formulas in Theorems 1, 2 and 3. Figure 2(b) further confirms the monotonicity property in Remark 1 and the prescribed range of capacity ratio for SZF described therein. Note also that in the small SNR region ($\rho < 0db$), MMSE delivers an impressive performance. However, the situation becomes very different when we consider a more practical SNR region. When $\rho > 0db$, SZF already outperforms other equalizers significantly. When the SNR reaches above $10db$, the SZF is very close to achieve full capacity.

To further confirm the capacity achieving property, $10,000$ tests were conducted, with $\mathbf{H}$ drawn from $\mathcal{C}^{8\times 6}$ Rayleigh-fading assembly. The channel condition is assumed to be generic, i.e. our

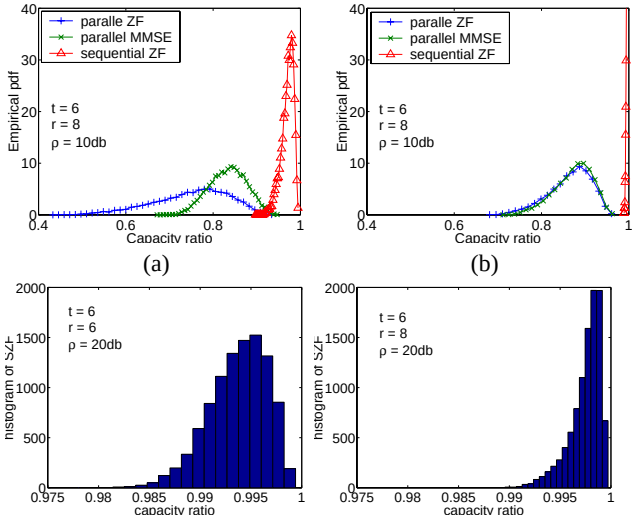

Fig. 3. Distribution of capacity ratios (based on $10,000$ tests) for parallel ZF, MMSE and sequential ZF equalizers at (a) $\rho = 10db$ and (b) $\rho = 20db$ for $\mathcal{C}^{8\times 6}$ MIMO channels. The $\rho = 20db$ SZF histograms for $\mathcal{C}^{6\times 6}$ and $\mathcal{C}^{8\times 6}$ MIMO channels are displayed in (c) and (d) respectively.

experiment excludes those ill-conditioned channels with

$$\frac{\min(|\lambda_i|^2)}{\max(|\lambda_i|^2)} \leq 0.01 = -20db.$$

Figure 3(a)(b) display the empirical pdf of capacity ratios achieved by the three equalizers at $\rho = 10db$ and $\rho = 20db$, respectively. At $\rho = 10db$, the average capacity ratios of parallel ZF, MMSE and SZF are about 74.96%, 83.34% and 97.07% respectively. For $\rho = 20db$, the three values are correspondingly 86.46%, 87.27%, and 99.75%. In both cases SZF significantly outperforms the others. It is worth noting that the performance difference between parallel ZF and MMSE goes down with increasing ρ. At $\rho = 20db$, their curves almost coincide, and the capacity ratio of SZF is densely located around 0.99 in the shape of an impulse function. Non-square MIMO channels with $r > t$, should outperform the square MIMO due to the expanded receiver diversity. This is confirmed in Figure 3(c)(d), which show the histograms of SZF equalizer for $10,000$ $\mathcal{C}^{6\times 6}$ and $\mathcal{C}^{8\times 6}$ Rayleigh-fading channels. It is evident that, in both cases, the SZF achieves nearly the full channel capacity.

5. REFERENCES

[1] A. J. Viterbi, *Spread Spectrum Multiple Access with Binary PSK Modulation Can Approach Shannon Capacity for the Aggregate Gausian Channel*, 1986, preprint.

[2] M. K. Varanasi and T. Guess, "Optimum Decision Feedback Multiuser Equalization with Successive Decoding Achieves the Total Capacity of the Gaussian Multiple-Access Channel", *Conference Record of the 31st Asilomar Conf. on Signals, Systems & Computers*, vol. 2, pp. 1405-1409, 1997.

[3] G.J. Foschini,"Layered Space-time Architecture for Wireless Communication in Fading Environments When Using Multiple Antennas",*Bell Labs Tech. J.*, pp.41-59, vol.2, 1996.